An Investigation of the Effect of Gaseous Fuel Inlet on the Design and Modelling of a Gas -Turbine Combustor for Heating Purposes

A. K. Azab[1], Tamer M. Ismail[2], M. M. Abd Alaal[3] M. A. Elkady[3]
[1]*Assistant Lecture, Department of Mechanical Engineering, Al-Azhar University, Cairo, Egypt.*
[2]*Associate Professor, Department of, Department of Mechanical Engineering, Suez Canal University, Ismailia, Egypt.*
[3]*Professor, Department of Mechanical Engineering, Al-Azhar University, Cairo, Egypt.*

(Corresponding author: A. K. Azab)

ABSTRACT: The target of a combustor design is to produce enough amount of hot gases at moderate temperature (900°C) for hearing purpose applications such as, heavy crude oil transportation. The combustor design selected is related to gas turbine combustion chamber family, for intensified combustion and moderate exit temperature. Such design can be suitable for using biofuels such as; biogas and biodiesel. It has been realized that, the inlet of the gaseous fuel highly affects the combustor performance parameters and flame length. Consequently, it is important to investigate the optimum gaseous fuel nozzle as it might be required to modify fuel inlet diameter to shorten the flame length in case of gaseous fuel while keeping the same combustor performance in case of biodiesel. The present study employed CFD design simulation as well as experimental proto type testing. The work was divided into two parts, the first one was carried out using biodiesel fuel, and the other was conducted using biogas. It is well known that, the combustion mechanism in the primary zone is responsible for the flame length elongation, which is transferred from flame stabilization by swirling action to flame stabilization by wake region resulting from high fuel jet velocity. High fuel jet velocity, shorten the available residence time in the primary zone. The present study investigates the effect of using various inlet gaseous fuel diameters to attain the optimum value suitable for enhancing combustor performance. Three gaseous fuel nozzle diameters (8, 11, and 16 mm) were selected with fuel velocities of 47.8, 25.3 and 12 m/s respectively.   The results of the present work include the temperature distribution, velocity vectors, velocity contours, flame length, and exhaust gases analysis. A comparison between experimental and theoretical results is also presented. The results reveal that, by increasing the gaseous fuel nozzle diameter the effect of fuel jet momentum becomes minor with respect to swirler tangential momentum which emphasis the flame anchoring in the primary zone. Accordingly, the overall flame length is reduced, while keeping high combustor performance. The NOx, and CO are increased slightly for the 8 mm fuel nozzle compared with larger nozzles. The attained good agreement between theoretical and practical model, indicates that the model can be applied for a wide range of design parameters.

Keywords: Combustor, Combustion Chamber, Biogas, Natural gas, Nozzle diameter.

Abbreviations: GHGs, greenhouse gases; PCM, phase changing material; SC, solar chimney; GCHE, ground coupled heat exchanger; EAHE, earth air heat exchanger; GSHP, ground source heat pump; PV, photo voltaic; HVAC, heating ventilation and air conditioning; AC, air conditioner; PBP, payback period.

I. INTRODUCTION

Biogas, as a sustainable energy, is considered one of the alternatives to fulfill energy needs because of the rapidly increase of power demands and availability limits of fossil resources [1]. Biogas has very wide range of resources such; public's solid waste, residuals effluent, and gasification. It can be helpfully utilized within the power production, heating systems and the like. It is basically composed of methane and carbon dioxide with a follow sum of hydrogen, sulfur, and nitrogen. The amount of these follow components is changed concurring to how the gasification and generation are done [2]. In this paper natural gas has been used as a gaseous fuel for the design of the combustor to produce around 100 kW thermal energy. The results can be applied also for biogas as biogas mainly consists of methane ~ 70%.

Great majority of gas turbine combustor utilizing biogas fuel are found in the literatures. Hosseini [3] designed

gas turbine (GT) power generation system integrated with a flameless boiler for steam generation for hydrogen production in a solid oxide steam electrolyzer. He reported the design performance of using biogas fuel (60% CH_4 + 40% CO_2). Liu *et al.,* [4] studied the impacts of fuel compositions, fuel injectors position and pilot split on combustion efficiency on a DLE (Dry Low Emissions) combustor designed for a micro-gas turbine. Chiong *et al.,* [5] inspected combustion characteristics of palm biodiesel/methyl esters (PME) and natural gas (NG) blend by using a model gas turbine swirl burner at vane angle (θ) 30°, 45° and 60°. Quintino *et al.,* [6] studied the effect of the CO_2 concentration (X_{CO2}) for different equivalence ratios (φ) on CH_4/CO_2/air (biogas) flames glow numerically and experimentally. Kahraman *et al.,* [7] investigated the possibility of hydrogen utilizing as an alternate fuel in the tubular combustor fueled by jet-A fuel. To achieve this objective, a numerical study was obtained for the combustion characteristics in the combustion chamber of a Rolls-Royce Nene turbojet

engine fueled by gas jet-A and at various air to fuel ratio for certain values of output thermal power.

Sher *et al.,* [8] executed a set of tests in a 20kWth fluidized bed combustor under oxy-fuel conditions firing two non-woody fuels (miscan thus and straw pellets) and one woody fuel (domestic wood pellet). Liu and Sanderson [9] inspected the impact of fuel heating value variation on combustion for a single standard Siemens SGT-300 7.9 MW dry low emission (DLE) combustor in a high pressure rig at literal engine operating conditions. Combustor flame performance plays vital role in the combustion stability and efficiency. Flame stability and high exhaust gases temperature are the main factors for increasing combustor performance. Abundant empirical and mathematical researches have been prepared on gas turbine combustor. Few of these researches are outlined.

Zhang *et al.,* [10] investigated the flame properties of SGT-100 combustor in three different mixing uniformities by Large Eddy Simulation (LES) coupled Flamelet Generated Manifold (FGM) model. Zhao *et al.,* [11] simulated the ignition procedure in a laboratory scale annular combustor with sixteen swirling injectors by using Large Eddy Simulation (LES) coupled with a detailed propane/air mechanism and Adaptive Mesh Refinement (AMR). Rau *et al.,* [12] investigated the effect of pressure increasing on the laminar flame velocity of biofuels and the relation between pressure and flame velocity. Liu *et al.,* [13] reported the gaseous fuel extension flexibility for an industrial gas turbine engine. Chen *et al.,* [14] proposed low emission combustion technology Based on RQL (rich-burn/quick-quench/lean-burn), a RP-3 fuelled high temperature rise combustor. Harish *et al.,* [15] investigated cross-flow non-premixed flames characteristics, where biogas is injected through a horizontal porous plate and air is blown parallel to the fuel injector. Patra *et al.,* [16] studied the changes in the flame characteristics and combustor performance in a cylindrical spray combustor when operated with kerosene and kerosene–ethanol blends. Saediamiri *et al.,* [17] reported an experimental work on the impact of the burner geometry on the stability limits of a turbulent non-premixed biogas flame. The study concentrated on the role of the low swirl strength of the co-airflow, and the fuel nozzle diameter. Medwell and Dally [18] investigated the usage of experimental techniques and laminar flame calculations for the role of hydrogen addition on the structure of the Moderate or Intense Low oxygen Dilution (MILD) combustion regime. Wilson and Lyons *et al.,* [19] reported experimental tests of biogas fueled combustors for turbulent, lifted, non-premixed flames in co-flow, and with dilution, with implications. Methane and ethylene; diluted by nitrogen was the used fuels.

In recent years, the main target has been to reduce engine pollutant emissions, in particular NOx, CO_2, and CO to meet the strict regulations. The most promising way to implement the acquiescence is reported to be lean combustion technology. Accordingly, large efforts have been done in developing a lean burning mixture mechanism for the combustion chamber applications.

Somarathne *et al.,* [20] investigated the emission productions of turbulent non- premixed ammonia (NH 3)/air and methane (CH 4)/air swirl flames through numerical simulations using large –eddy simulations with the finite-rate chemistry technique. Innocenti *et al.,* [21] conducted a theoretical analysis pollutant emissions prediction in a tubular combustor for aero-engine applications by a hybrid CFD-Chemical Reactor Network (CRN) approach. Chong *et al.,* [22] reported soot formation in a model aircraft engine configuration operating at elevated pressures by large eddy simulation (LES) and detailed models for precursor and soot population evolution. Mordaunt and Pierce [23] designed a combustion device and studied the impact of rising levels of CO_2 as a supplement to the combustion of pure CH_4 with air. Madhiyanon *et al.,* [24] analyzed the performance of combustion and thermal efficiency, volumetric combustion intensity, and pollutant emissions of developed a novel cyclonic fluidized-bed combustor for burning rice husk.

The main objective of the present work is to design a combustion chamber using gas turbine combustor main features and to be able to supply efficiently both liquid or gaseous fuels, to be used in heating purposes (large quantities of hot gases with moderate temperature ~ 900°C). However, the present study is concerned with the gaseous fuel inlet design to get the required flame characteristics to be suitable for the required applications.

II. EXPERIMENTAL TEST RIG

In this study the experimental work was made to validate the numerical model that is because the difficulty of validation with another numerical models indicated in the literatures where, the geometry, boundary conditions, and combustion models are different from model to model. The experimental test rig will be simplified in following schematic diagram shown in Fig. 1. Fig. 1 illustrate schematic diagram of the experimental test rig. The test rig consists of 27 part each part is identified in Table 1. The function of each part is summarized in this list.

III. COMPUTATIONAL MODEL

A model was developed through CFD analysis to achieve the optimum design of the combustor for proper mixing and penetration of combustion elements in the primary, secondary, and dilution zones to achieve high combustion efficiency and uniform exit temperature. During this process, it was ensured that the total pressure remained almost the same. The modeling began with the design of the combustor geometry by using design modeler, followed by combustor mesh and boundary conditions, and ended with finite element model. The combustor geometry for analysis is a can combustor having an axial flow swirler with 12 aero foil shape vanes at the inlet of combustor, provided to maximize the inlet air turbulence. An injector with 6 holes of 5 mm diameter is attached at the entrance of the primary zone. The length of the liner and number of holes on the liner are designed accordingly and all the dimensions and combustor specifications are provided in Table 2 and 3 Fig. 2 shows the cross-sectional view of the combustor which is designed according to the design methodology [4].

Analysis was carried out using ANSYS FLUENT 15. The parametric geometry model was built in ANSYS Design Modeler and consisted of a swirl and combustor liner.

Swirl blade was built using three cross- sections (blade profile on the hub, the middle and peripheral diameter). Results obtained through computation show proper mixing of combustion products with the admission of air through different zone holes and almost uniform temperature at exit.
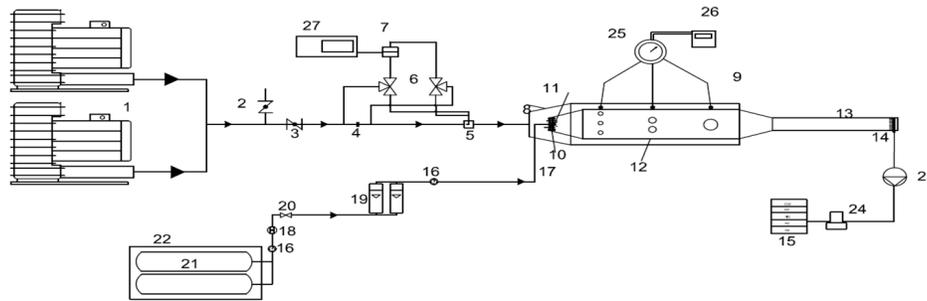
Fig. 1. Schematic diagram of experimental test rig.

Table 1: Test rig symbols description

S.No.	Symbol	Description
1.	Ring Air Blower	Two blowers are obtained to provide pressurized air. $Q_{max} = 6.3$ m^3/min $P_{max} = 45$kPa
2.	Air Bypass	Bypass air flow control of diameter 2.5in and butter fly valve to prevent back pressure to blowers.
3.	Air Control Valve	Main air flow throttling valve to control on air flow. N.D.= 2.5 in
4.	Orifice Plate	Equipped with calibrated differential pressure transducer to measure air flow.
5.	Pitot Tube	Differential pressure pitot tube, equipped with calibrated differential pressure transducer to measure air flow. probe N.D.= 8 mm - pipe N.D. = 2.5in
6.	Three-way Selectors Valves	To adjust measuring instrument easily.
7.	Pressure Transducer	Differential pressure transducer to measure air flow rate.
8.	Combustor outer casing	Working as a cooling jacket around the liner. L= 540 mm - D= 102 mm.
9.	Thermocouples	3 thermocouples of bare peat type K, to measure cooling air temperature. wire diameter = 0.2 mm
10.	Swirler	With 12 vane and hup outer diameter of 70 mm and inner diameter of 20 mm.
11.	Fuel nozzle	With a rated capacity of 1.5 GPH at a pressure difference of 7 Bar. This fuel nozzle is sufficient for the case study as it produces a solid spray of fuel with 45° angle.
12.	Combustor liner	Dimensions of L= 500 mm, D= 90 mm ended with exit nozzle of 90 mm to 60mm diameter. Required air for combustion process provided from two entering points 25% of the total air path from the swirler and 5% of total air path through 6 holes of 5 mm diameter at the primary zone.70% from total entering air to combustor divided to 20% from the total air entering through 8 holes of 8 mm diameter at the secondary zone and 50% from the total air entering through 10 holes of 12 mm diameter at the dilution zone.
13.	Measurement Tube	With dimensions of L= 800 mm, D= 60mm pipe to convert turbulent flow to laminar flow for enhancing measuring technique.
14.	Water cooled average sampling probe	Sample line was made of black steel pipe with 60 mm of length to produce fully developed flow of exhaust gases. Sampling probe consists of 4 mm internal diameter stainless steel tube drilled with 4 holes of 2 mm diameter each to collect gases from pipe.
15.	Dry gas analyzer	An ADC infrared multi-gas analyzer unit, model MGA3000 and CAI total hydrocarbon analyzer (THA), model 600 FID were used for measuring emissions resulted from the combustor during operation under various conditions. The major exhaust gas components measured in the present study were nitric oxide (NO), carbon dioxide (CO_2), carbon monoxide (CO), oxygen (O_2) and unburned hydrocarbon (UHC).
16.	Fuel Pressure Gauge	To indicate gas pressure.
17.	Fuel Feed Line	Feeding fuel line of combustor nozzle.
18.	Pressure regulating valve	To reduce exit pressure of gas cylinder from 200 bar to 1.2 bar.
19.	Fuel Flow Meter with needle valve	To indicate gas flow rate and control on the flow.
20.	Fuel Valve	To control on gas flow.
21.	Gas cylinder	Two gas cylinders capacity of 70m3 and pressure of 200 bar.
22.	Gas cylinders table	To withstand gas cylinders and its control accessories.
23.	Gas Sampling Pump	A diaphragm pump provides exceptional quality, reliability, affordability, 100% oil-free, contamination free, corrosion resistant, and leak free sampling.
24.	Sampling Gas Chiller	Enhance fuel gas quality by eliminating condensate, and controlling the temperature.
25.	Thermocouple selector switch	Selector utilized to select the trip point temperature to be obtained. The chosen temperature is constantly obtained through.
26.	Temperature Indicators	Used to indicate the system overheating or an abnormal condition of system.
27.	Pressure indicator	With a sensing element, transmitting, and recording devices for measuring and recording pressure changes.

IV. GOVERNING EQUATIONS

It is well known that; six equations should be solved to model the flow field. These equations are continuity, momentum, energy, species transport, turbulence, and combustion equations. In the current investigation, flow is assumed to be steady, turbulent, compressible and reacting. The governing Navier-Stokes equations (RANS) for the conservation of mass, momentum, energy, and species concentration for the gas, together with an equation of state are approximated for each mesh cell. The resulting set of equations is solved numerically to obtain the flow field, mixing and combustion data. Table (4) shows the computational model for the combustor analysis.
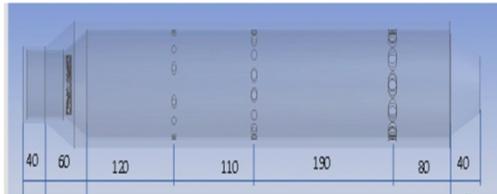
Fig. 2. Geometry of the liner of the combustor (All dimensions in millimeters)

V. NATURAL GAS AS A FUEL OF COMBUSTOR

Natural gas was used as a combustor fuel; the characteristics of the fuel are shown in Table 5 [25]. The incoming air at the specified pressure and temperature enters into the combustion chamber through liner holes, then, reacts with the jet of biogas fuel. The effect of providing aero foil swirler at the inlet on flow field and on the combustor, performance will be discussed.

Table 2: Dimensions of various parts of combustor.

Part	Dimensions
Hub Diameter, D_{hub}	70 mm
Swirl Diameter, D_{sw}	20 mm
Swirl No., S_N	1.16
D_{sw}/D_{hub}	0.29
Liner length, L_L	500 mm
Liner Diameter, D_L	82 mm
Case Length	540 mm
Case Diameter	102 mm

Table 3: Specifications of the combustor.

Design parameter	Value
Liner diameter	102 mm
Fuel flow rate	0.002304 kg/s
Inlet fuel temperature	350 K
Number of primary holes	6
Diameter of primary holes	5 mm
Number of secondary holes	8
Diameter of secondary holes	8 mm
Number of dilution holes	10
Diameter of dilution holes	12 mm
Total inlet air flow rate	0.126 kg/s
Primary holes FOA	5 %
Secondary holes FOA	20 %
Dilution holes FOA	50 %
Swirler FOA	25 %
Inlet air temperature	350 K
Inlet air pressure	120 kPa
Inlet air from swirler	0.0315 kg/s

Table 4: Computational mode.

Fluid model	Thermal energy
Turbulence model	k-ε
Species Model	Non premixed combustion
Radiation model	Discrete Ordinates
Discrete phase model	Interaction with continuous phase

Table 5: Natural gas fuel analysis [25].

Analysis Parameter	Value	Remarks
Boiling point	-161.5^{o}C	At 1 atm
Freezing point	-182.5^{o}C	At 1 atm
Specific gravity	0.43 to 0.47	Related to water = 1
Gas density	0.7 to 0.9 Kg/m^3	At STP
Flammability limits	4 to 15	By volume in air
Carbon content	73	By weight
Hydrogen content	24	By weight
Oxygen content	0.4	By weight

VI. MODEL VALIDATION

The validity of the present modelling outputs data was attained using the experimental measurements of hot gases produced from the designed combustor. The simulation, was carried out using CFD 3D computational model with a structured grid composed of 1575471cells. The fuel used in the present study is biodiesel. The results presented in following figures obtained a close relationship between both results.

Fig. 3 shows the comparison between computed and experimental results of average temperatures at the combustor exit for variable inlet fuel nozzle diameter. From Fig. 3 it is shown that good agreement between both results, with the same trend of curve.
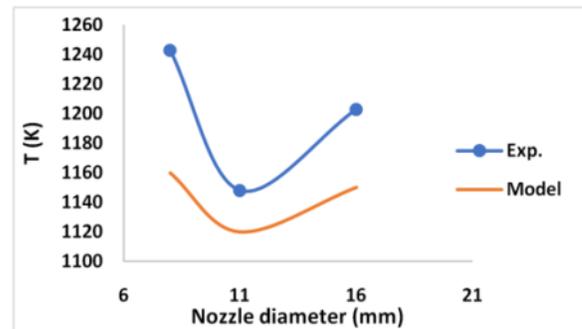
Fig. 3. Comparison of the exit temperature at present model and present experimental.

Figs. 4 and 5 indicate the mole fraction of CO_2 and O_2 at the exit of combustor resulting by the present theoretical model and the present experimental proto type. Although, there is some discrepancy for some values, model output results close to the experiment, at combustor exit. Therefore, the applied model gives good prediction for the species.
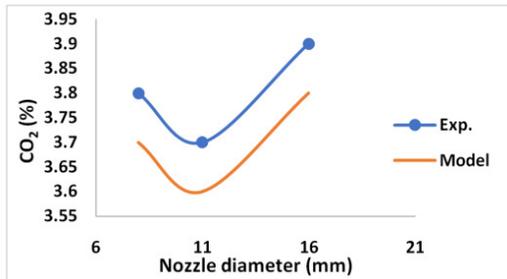
Fig. 4. Comparison of mole fraction of CO_2 emission from present model and present experimental.
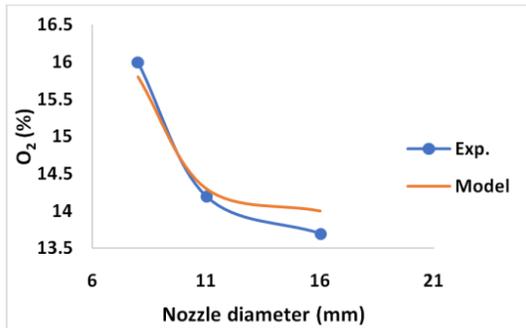
Fig. 5. Comparison of mole fractions of O_2 emission from present model and present experimental.

Experimental Results. Fig. 3 illustrates the effect of the inlet fuel nozzle diameter on the exit gases temperature from the combustor (T_{out}) for the combustor rated load of 100 kW. It is worth noting that, the variation of nozzle diameter changes the fuel inlet velocity while keeping the inlet fuel flow rate constant. This means that with larger nozzle diameter the fuel flow velocity inside the combustor becomes low i.e. the tangential momentum of the swirler becomes the dominant and hence flame stabilization by swirling action is done. This increasing the reactions residence time, and short anchored flame. On the other hand, the volume of the combustor is constant which means that, the ratio of absorption of the heat by the metal to the generated heat by combustion is increased. By decreasing the nozzle diameter, the reactions residence time reduced and the heat liberated increased. In this case the system shall have a point where the optimum results are achieved from the point of view of temperature levels. The present optimum nozzle diameter is between 11 and 16 mm which achieve the required output temperature. The difference between the minimum and maximum temperatures was about 100°C.

Fig. 4 shows the variation of percentage CO_2 emissions produced from the designed combustor with different values of inlet nozzle diameter and rated load of 100 kW. It is obvious that, the percentage CO_2 emissions produced from the combustor decreases with the increase inlet fuel nozzle diameter, till a nozzle diameter of 11 mm, then the percentage of CO_2 emission starts to increase by about 0.15 % with the increase in nozzle diameter. This means that the combustion efficiency increased with fuel velocity decreased. This may be explained as some CO_2 dissociation has been occurred. Figure (5) illustrates the effect of the fuel nozzle diameter on percentage of O_2 emission produced from the designed combustor. From the plotted lines it is

clear that, the percentage of O_2 emissions produced from the combustor decreases with the increase of inlet fuel nozzle diameter i.e. the rate of O_2 consumption is increased due to better combustion. This may be explained as the swirling action is strong enough to finish most of the combustion in the primary zone and the secondary zone air oxidize the remaining HC from primary zone.

VII. MODEL RESULTS AND DISCUSSION

The present study is a trial to apply the combustion technology, which is used in gas turbine in heating purposes, due to its high combustion efficiency, low emissions, intensified combustion, high power, and relatively small size. Therefore, a combustion chamber has been designed theoretically and an experimental model has been done. The project target is to use fossil or biofuels, liquid or gaseous. To switch on between liquid or gaseous the fuel nozzle shall be exchanged. It is required to keep the combustor performance the same for both types of fuels, therefore the gaseous fuel nozzle should be designed precisely due to the high volume flow rate of gaseous with respect to liquid fuel for the same power, the gaseous fuel jet can reach a velocity of 150 m/s which is high enough to disturb the swirler effect.

A three gaseous fuel nozzles have been designed and investigated in both theoretical and experimental study. The three fuel nozzle diameters are 8, 11, and 16 mm, which give fuel velocity of values 47.8, 25.3, and 12 m/s respectively. The results include the temperature contours, velocity contours, velocity vectors, (CO_2, CO, O_2, HC, and NOx) gas analysis contours, and average temperatures at combustor sections.

The results shown in Fig. 6 reveal that the temperature in case of 8 mm nozzle diameter is axisymmetric and the high temperature zone has been elongated to the secondary liner holes, while in cases of 11 and 16 mm the high temperature zone become in burner side and its length is short. This can be explained as the fuel jet velocity increased the gaseous fuel momentum increase and become more than the tangential momentum of the swirler. This results in attenuating the swirler effect. This also can be observed from Fig. 7 which indicates the velocity contours. It is noted from Fig. 7 that the 8 mm nozzle increases the fuel jet velocity to be more than 100 m/s, as well as the swirler action is not noticeable.
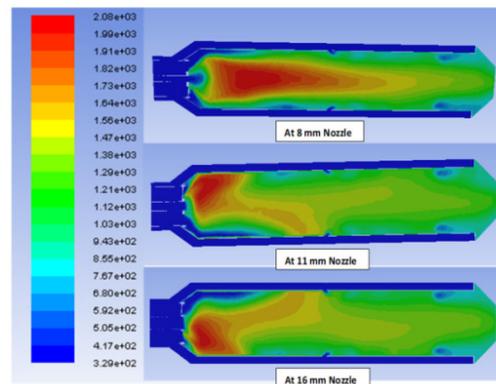
Fig. 6. Temperature contours at different fuel nozzle diameter.
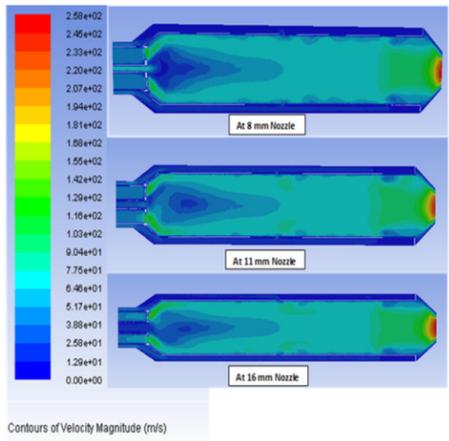
Fig. 7. Velocity contours at different fuel nozzle diameter.

As the fuel jet velocity increases a region of negative pressure around the nozzle is initiated (wake region) and a central zero velocity, this region is strong enough to suction part of the swirler air to be recirculated around the nozzle axial, this can be observed in Fig. 8 which indicates the velocity vectors. In case of 11 and 16 mm diameters the effect of the swirler is more dominant therefore the tangential component directed the flow tangentially.

The increase of fuel jet velocity can change the combustion stability and combustion mechanism, from swirl to wake region. Also, as the fuel jet increases there is a tangential shear layer between the fuel jet and the surrounding air layer, this help the fuel air mixing and fuel air reaction.

From the above-mentioned discussions one can conclude that if the fuel jet increases than certain limit the combustion mechanism will transfer from swirl to wake and tangential shear layer mechanism will yield different flame characteristics. The flame will increase in length and will disturb the secondary holes effect as shown in Fig. 8 of velocity vectors.
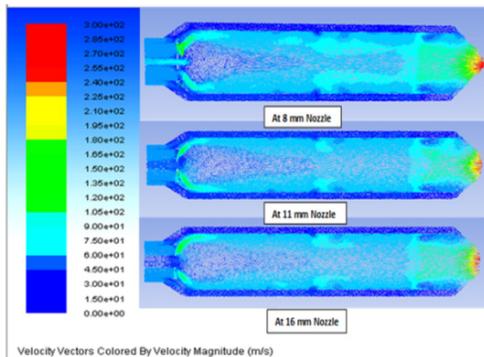
Fig. 8. Velocity vectors at different fuel nozzle diameter.

Figs. 9, 10, 11, and 12 illustrate the gas analysis contours profiles for the components CO_2, O_2, CO, and HC. It is noted that the maximum value of CO_2 concentration for 8 mm nozzle is located at the combustor center line and its length is long compared with higher nozzles diameters. In the other hand the 11mm and 16mm nozzles indicate that the maximum CO_2 concentrations located in the combustor side and

smaller region in size. These is due to the effect of the swirling effect which able to nearly complete in the primary zone, while the 8 mm nozzle diameter extend the combustion to the secondary zone and elongate the flame length.
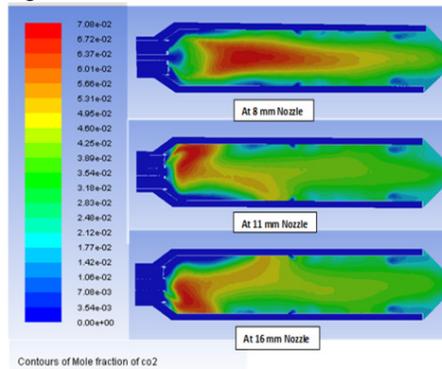
Fig. 9. Mole fraction contours of (CO_2) at different fuel nozzle diameter.

The same observation can be seen from Fig. 10 which indicates the O_2 concentration contours in combustor cross section, i.e. the minimum concentration value of O_2 are located in the combustors side due to swirl action. The temperature, CO_2, and O_2 are all indication to the behavior of the combustion process as well as the location on maximum heat release rates. It is also noted that the areas of O_2 in the primary zone for 8 mm nozzle are larger than that of larger nozzles which indicate that the flame extend its reaction to reach the secondary.
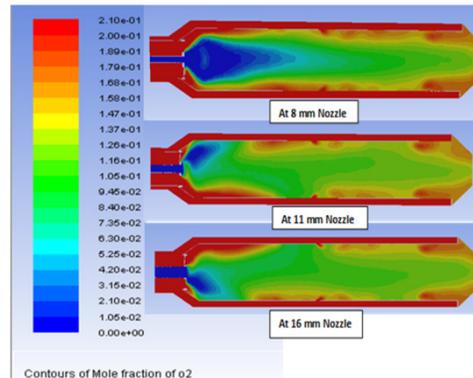
Fig. 10. Mole fraction contours of (O_2) at different fuel nozzle diameter.
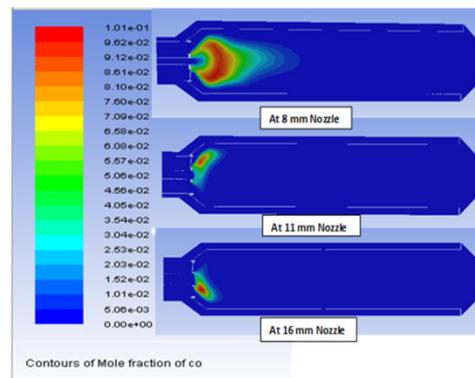
Fig. 11. Mole fraction contours of (CO)at different fuel nozzle diameter.
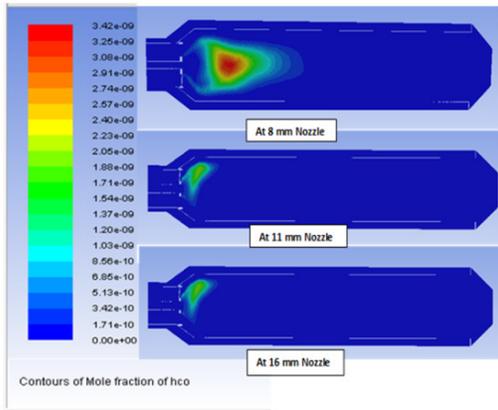
Fig. 12. Mole fraction contours of (HC)at different fuel nozzle diameter.

Fig. 13 presents the NOx emissions as a longitudinal section contour. The main amount of NO_x formation is due to thermal NOx, where NO_x generated by the combustion of fuels is primarily controlled by the Zeldovich mechanism. The rate of formation of thermal NO_x is highly temperature dependent. Therefore, the technical direction for minimizing NO_x formation is to reduce temperature in the flame zone. Therefore, and according to the temperature map inside the combustor the maximum temperatures were attained in the primary zone as indicated in for nozzle diameters of 11mm and 16mm. However, for 8mm nozzle diameter the maximum temperature at the primary zone but the maximum amount of NO_x start at dilution zone this is because the flame speed at primary zone very high the formation mechanism of NO_x can't find enough time to generate at primary zone and start at dilution zone.
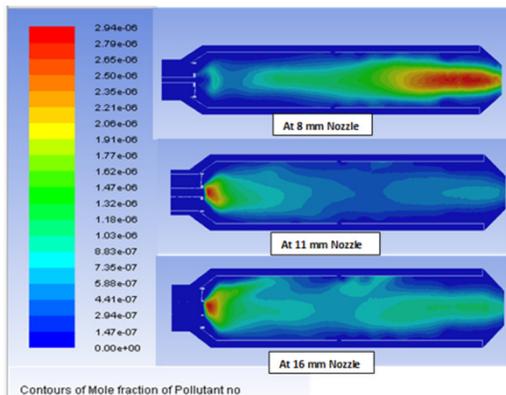
Fig. 13. Mole fraction contours of (NO_x) at different fuel nozzle diameter

VIII. CONCLUSIONS

The following conclusions could be deduced from the course of the present investigation:
— Gas turbine combustor can be used in heating purposes efficiently due to its high combustion efficiency, compact size, intensified combustion, moderation hot gases temperature, and low pollutant emissions.
— The modeling of gas turbine combustor using CFD simulation tools gives good agreement with the experimental results which recommended for such designs.

— The suitable selection of the gaseous fuel nozzle is considered major combustion parameter in the design process.
— To get good simulation results it is mandatory to adjust some combustor parameters from the experimental tests.
— The fuel nozzle design can change the combustion characteristics therefore the selection of the fuel nozzle according to the application is essential.

IX. FUTURE SCOPE

This study was carried out theoretically and experimentally for the effect of gaseous fuel nozzle diameter on the combustion process of gas turbine, to get a better understanding of the its impact under different parameters. Now based on the outcomes of this study, we have the future plan and suggestions for next researches related to the usage of biogas fuel for gas turbine combustor. The current study will be quite helpful to understand the vital effect of the nozzle selection on the flame and emissions produced from gas turbine combustor, this study can contribute in the future by applied the concept on different types of gaseous fuel. This study is also helpful to make a reliable relation between the geometry of combustor, rated output thermal power from combustor, and gaseous fuel nozzle diameter.

Conflict of Interest. The authors confirm that there are no known conflicts of interest associated with this Publication of this paper.

REFERENCES

[1]. Liu, H., Wang, Y., Yu, T., Liu, H., Cai, W., & Weng, S. (2020). Effect of carbon dioxide content in biogas on turbulent combustion in the combustor of micro gas turbine. *Renewable Energy, 147,* 1299–1311. https://doi.org/10.1016/j.renene.2019.09.014.
[2]. Sahin, M., &Ilbas, M. (2020). Analysis of the effect of H₂O content on combustion behaviours of a biogas fuel. *International Journal of Hydrogen Energy, 45*(5), 3651–3659. https://doi.org/10.1016/j.ijhydene.2019.02.042
[3]. Hosseini, S. E. (2020). Design and analysis of renewable hydrogen production from biogas by integrating a gas turbine system and a solid oxide steam electrolyzer. *Energy Conversion and Management, 211*, 112760.
https://doi.org/10.1016/j.enconman.2020.112760.
[4]. Liu, A., Yang, Y., Chen, L., Zeng, W., & Wang, C. (2020). Experimental study of biogas combustion and emissions for a micro gas turbine. *Fuel, 267*, 117312. https://doi.org/10.1016/j.fuel.2020.117312.
[5]. Chiong, M. C., Valera-Medina, A., Chong, W. W. F., Chong, C. T., Mong, G. R., & Mohd Jaafar, M. N. (2020). Effects of swirler vane angle on palm biodiesel/natural gas combustion in swirl-stabilised gas turbine combustor. *Fuel, 277*, 118213. https://doi.org/10.1016/j.fuel.2020.118213.
[6]. Quintino, F. M., Trindade, T. P., & Fernandes, E. C. (2018). Biogas combustion: Chemiluminescence fingerprint. *Fuel, 231*, 328–340. https://doi.org/10.1016/j.fuel.2018.05.086.
[7]. Kahraman, N., Tangöz, S., &Akansu, S. O. (2018). Numerical analysis of a gas turbine combustor fueled by hydrogen in comparison with jet-A fuel. *Fuel, 217*, 66–77. https://doi.org/10.1016/j.fuel.2017.12.071.

[8]. Sher, F., Pans, M. A., Sun, C., Snape, C., & Liu, H. (2018). Oxy-fuel combustion study of biomass fuels in a 20 kWth fluidized bed combustor. *Fuel, 215,* 778–786. https://doi.org/10.1016/j.fuel.2017.11.039.

[9]. Liu, K., & Sanderson, V. (2013). The influence of changes in fuel calorific value to combustion performance for Siemens SGT-300 dry low emission combustion system. *Fuel, 103*, 239–246. https://doi.org/10.1016/j.fuel.2012.07.068.

[10]. Zhang, Z., Liu, X., Gong, Y., Li, Z., Yang, J., & Zheng, H. (2020). Investigation on flame characteristics of industrial gas turbine combustor with different mixing uniformities. *Fuel, 259*, https://doi.org/10.1016/j.fuel.2019.116297.

[11]. Zhao, D., Xia, Y., Ge, H., Lin, Q., & Wang, G. (2020). Large eddy simulation of flame propagation during the ignition process in an annular multiple-injector combustor. *Fuel, 263*, 116402. https://doi.org/10.1016/j.fuel.2019.116402.

[12]. Rau, F., Hartl, S., & Hasse, C. (2019). Numerical and experimental investigation of the laminar burning velocity of biofuels at atmospheric and high-pressure conditions. *Fuel, 247*, 250–256. https://doi.org/10.1016/j.fuel.2019.03.024.

[13]. Liu, K., Sadasivuni, S., & Parsania, N. (2019). Industrial gas turbine engine response and combustion performance to fuel changeovers in compositions and heating values. *Fuel, 242*, 507–519. https://doi.org/10.1016/j.fuel.2019.01.030.

[14]. Chen, J., Li, J., Yuan, L., & Hu, G. (2019). Flow and flame characteristics of a RP-3 fuelled high temperature rise combustor based on RQL. *Fuel, 235*, 1159–1171. https://doi.org/10.1016/j.fuel.2018.08.115.

[15]. Harish, A., Rakesh Ranga, H. R., Babu, A., & Raghavan, V. (2018). Experimental study of flame characteristics and stability regimes of biogas – Air cross flow non-premixed flames. *Fuel, 223*, 334–343. https://doi.org/10.1016/j.fuel.2018.03.055.

[16]. Patra, J., Ghose, P., Datta, A., Das, M., Ganguly, R., Sen, S., & Chatterjee, S. (2015). Studies of combustion characteristics of kerosene ethanol blends in an axi-symmetric combustor. *Fuel, 144,* 205–213. https://doi.org/10.1016/j.fuel.2014.12.036.

[17]. Saediamiri, M., Birouk, M., & Kozinski, J. A. (2014). On the stability of a turbulent non-premixed biogas flame: Effect of low swirl strength. *Combustion and Flame, 161*(5), 1326–1336. https://doi.org/10.1016/j.combustflame.2013.11.002.

[18]. Medwell, P. R., & Dally, B. B. (2012). Effect of fuel composition on jet flames in a heated and diluted oxidant stream. *Combustion and Flame, 159*(10), 3138–3145. https://doi.org/10.1016/j.combustflame.2012.04.012.

[19]. Wilson, D. A., & Lyons, K. M. (2008). Effects of dilution and co-flow on the stability of lifted non-premixed biogas-like flames. *Fuel, 87*(3), 405–413. https://doi.org/10.1016/j.fuel.2007.05.012.

[20]. Somarathne, K. D. K. A., C. Okafor, E., Hayakawa, A., Kudo, T., Kurata, O., Iki, N., & Kobayashi, H. (2019). Emission characteristics of turbulent non-premixed ammonia/air and methane/air swirl flames through a rich-lean combustor under various wall thermal boundary conditions at high pressure. *Combustion and Flame, 210,* 247–261. https://doi.org/10.1016/j.combustflame.2019.08.037.

[21]. Innocenti, A., Andreini, A., Bertini, D., Facchini, B., & Motta, M. (2018). Turbulent flow-field effects in a hybrid CFD-CRN model for the prediction of NOx and CO emissions in aero-engine combustors. *Fuel, 215*, 853–864. https://doi.org/10.1016/j.fuel.2017.11.097.

[22]. Chong, S. T., Hassanaly, M., Koo, H., Mueller, M. E., Raman, V., & Geigle, K. P. (2018). Large eddy simulation of pressure and dilution-jet effects on soot formation in a model aircraft swirl combustor. *Combustion and Flame, 192,* 452–472. https://doi.org/10.1016/j.combustflame.2018.02.021.

[23]. Mordaunt, C. J., & Pierce, W. C. (2014). Design and preliminary results of an atmospheric-pressure model gas turbine combustor utilizing varying CO_2 doping concentration in CH_4 to emulate biogas combustion. *Fuel, 124,* 258–268. https://doi.org/10.1016/j.fuel.2014.01.097.

[24]. Madhiyanon, T., Lapirattanakun, A., Sathitruangsak, P., & Soponronnarit, S. (2006). A novel cyclonic fluidized-bed combustor (ψ-FBC): Combustion and thermal efficiency, temperature distributions, combustion intensity, and emission of pollutants. *Combustion and Flame, 146*(1–2), 232–245. https://doi.org/10.1016/j.combustflame.2006.03.008.

[25]. Eswara, A. K. (2014). Introduction to natural gas: A comparative study of its storage , fuel costs and emissions for a harbor tug List of Symbols. *The Annual Meeting of Society of Naval Architects & Marine Engineers (SNAME)* on 8th November, 2013 at Bellevue, Washington, USA.https://www.researchgate.net/publication/262691939